Device for Non-Destroyable Monitoring with Magnetic Method of Welded Joints of Main Gas and Oil Pipelines

A.A. SEDYKH, A.N. KOVALENKO, S.V. MAKAROV, OAO Avtogaz, Moscow, Russia.

Abstract. The present article deals with the problem of detection of defects in the welded joint. The problem is redoubled due to the fact that the magnetic field above the welded joint is heterogeneous. Models of the welded joint and models of welded joint defects have been described. The limit of magnetic method for welded joints monitoring usage has been defined.

Introduction

There is a need for device for express analysis of annular and longitudinal welded joints when making welding works in a field conditions, constructing pipelines and re-isolating of pipelines. To provide these works the DKDT OAO "Avtogaz" experts have created a scanning magnetic device for non-destroyable monitoring of welded joints, hereinafter referred to as scanner.

Magnetic scanners "SkM-Sh" are intended for searching magnetic anomalies in annular and longitudinal welded joints and joints zones (cleaned from isolation, local rolls and welding spatters). Scanners are used for monitoring gas, oil and oil products transportation pipes made from ferromagnetic steel and alloys followed by determining the kind and parameters (size) of the defects (defective zones).

Method of registration of magnetic fields dispersing created by defects has been realized for monitoring by magnetic scanner. During the monitoring the monitored site is being magnetized by constant magnetic field. The device is being moved along the joint of the pipeline during the monitoring. The width of the monitored zone is 50 mm. The magnetic relief of the field near the surface of the monitored make is being measured by matrix of magnetic sensor converters, so called Hall sensor. The information during the monitoring is recorded on a flash-disc. The data from flash disc is then moved to PC. The operator using the software processes the received relief of magnetic field above the defective zone and determines the kind of defect, and afterwards its parameters: depth and linear sizes.

Scanner provides stable and proved picking-up information when being hand-moved along the pipe's circle at a speed of 0.5 m/sec.

The following defects can be determined by scanner: all kind of pores, slag inclusions, cold weld (poor penetration) longitudinal surface and inner cracks of welded joint. Minimal size of determined defect such as a pore is 1 mm in diameter with the tube's wall thickness not more than 4 mm. In all other cases maximal pore diameter should not exceed 0.25*T, but not more than 3 mm, where T is a tube's wall thickness. Maximal wall thickness Tmax=17 mm.

The deviation in determining the coordinate of the defect of defective zone is no more than:

- related to the pipe's circle – arch distance- +/- 1 mm from the monitoring start-point;
- related to the width of the monitored zone- +/- mm from the monitoring start-point.

Results

In order to determine parameters of defects one should necessarily know the inverse fields distribution above them in welded joint.

The analysis of the inverse fields distribution above the welded joint and in the strengthened zone showed that the particularities of welded joints are determined by the welding kind and method, steel type, joint and seam type. This knowledge allows to highlight those particularities of welded joints which significantly influence magnetic features of welded joints as well as the possibility to diagnose integrity defects in it using the methods magnetic fields inversing. The main features are the following:

- type of the welded joint strengthening;
- type of joint and type of seam;
- nonhomogeneity of chemical composition, metal structure and texture in different zones of welded joint;
- presence of residual weld tensions.

Due to the fact that the measuring system of magnetic field (in our case Hall sensors) is influenced during the magnetic monitoring by superposition of the applied field $H_{\tau 0}$, welded joint strengthening field – $H_{\tau p}$ and defect field - $H_{\tau d}$, the main task of this work is the theoretical and experimental research of the above mentioned fields and their superposition, which will provide reliable detecting the defects in welded joints.

In the work by Sharova A.M. and Novikov V.A. "the new method of increasing sensibility of MGK of one-side welded joints", MinAtom (Nuclear Energy Ministry), 1978, the influence of welded joints on a possibility detecting the defects of integrity has been distributed for the following groups:

1. Type of seam strengthening.
2. Nonhomogeneity of chemical composition and structure.
3. Nonhomogeneity of residual weld tensions distribution.
4. Nonhomogeneity of texture in different zones of welded joint.

Taking in consideration all the features of welded joint magnetizing the resulting field $\mathbf{H_n}$ on the surface of the seam is determined by superposition of the applied field $\mathbf{H_0}$, the field of welded joint strengthening $\mathbf{H_p}$, defect field $\mathbf{H_d}$, the fields of chemical $\mathbf{H_{ch}}$ and structural $\mathbf{H_{st}}$ nonhomogeneity, and also fields caused by residual weld tensions $\mathbf{H_\sigma}$, and nonhomogeneity of texture –$\mathbf{H_T}$:

$$\mathbf{H_n = H_0 + H_p + H_d + H_{ch} + H_{st} + H_T.}$$

As the analysis of welded joints features shows, welded joints may be divided into several groups where the number of components of the field $\mathbf{H_n}$ will be significantly less.

Thus when welding low-alloyed steel 09G2C with the wire Св-08G2C in CO_2 we have practically identical chemical composition and therefore there is no in such a joint any nonhomogeneity of structure because steel doesn't harden, and there is also no textural nonhomogeneity in different zones of welded joint. Residual tension always presents in welded joint, but with the help of negative hardening it can be significantly reduced. So, with the absence of defect:

$$\mathbf{H_n = H_0 + H_p.}$$

When welding low-alloyed tempered steel 15H1N1F and choosing the proper wire we can reach identity of chemical composition of the welded joint and $\mathbf{H_0}$ will be determined mainly by structural nonhomogeneity in the thermal influence zone.

Taking in consideration the above mentioned the following correspondences of $\mathbf{H_p}$ magnetic field inverse in the welded joint zone have been received in OAO "Avtogaz". (Fig.1)

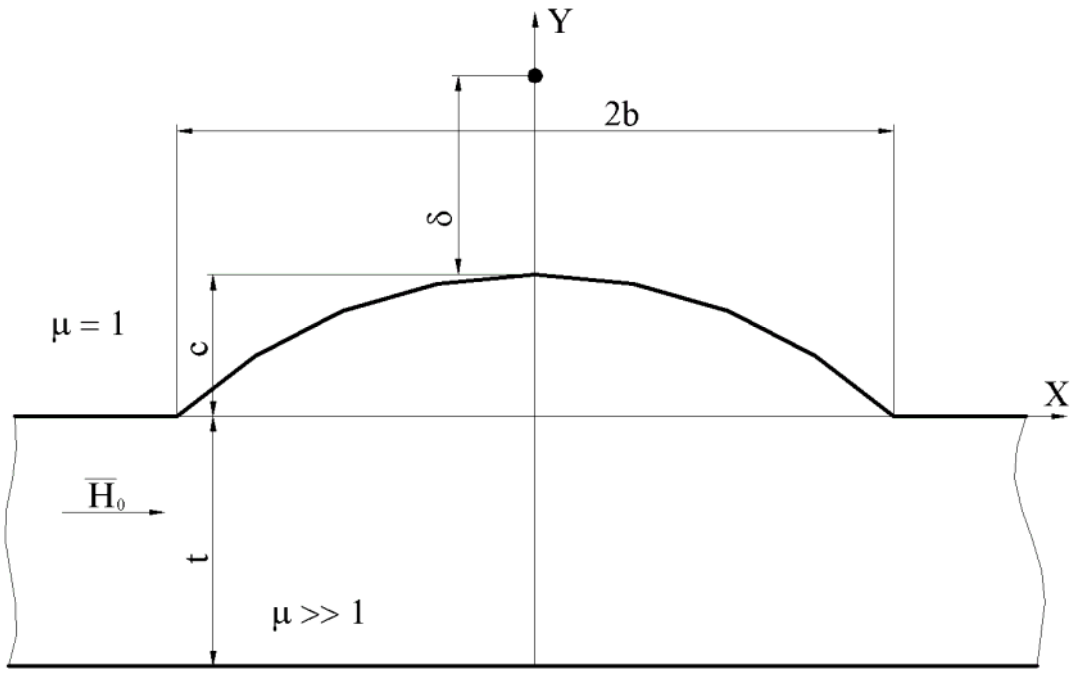

Fig.1

where 2b – width of the strengthening welding joint bead,
c - height of the strengthening welding joint bead,
t – pipe's wall thickness,
δ - height of monitoring point.

$$\frac{H_\tau}{H_0} = \frac{\frac{b^2}{2\cdot c} - \frac{c}{2} - \sqrt{\left(\frac{b^2}{2\cdot c} + \frac{c}{2}\right)^2 - x^2}}{t + \sqrt{\left(\frac{b^2}{2\cdot c} + \frac{c}{2}\right)^2 - x^2} - \frac{b^2}{2\cdot c} + \frac{c}{2}}$$

Distribution of magnetic field tangential component (H_τ) above the welded joint in correspondence of the height strengthening welding joint bead is shown on Fig.2.

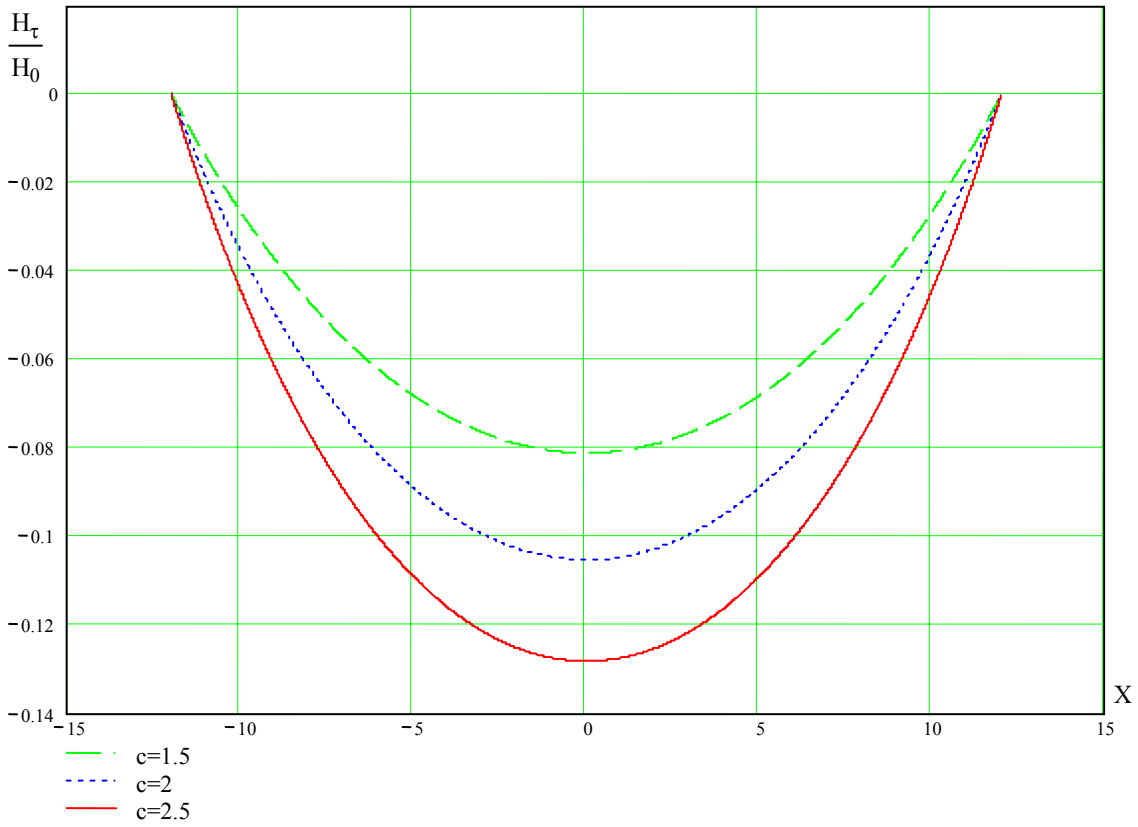

Fig.2. When 2b = 24 mm, t = 17 mm, c = 1.5, 2 и 2.5 mm, b> x >-b.

From Fig.2, distribution of $H_\tau(x)$ on the surface is the U – shape curve, with its minimum in the bead's symmetry platitude. In this work the influence of the wall thickness and height of the strengthening welding joint bead on the value (H_τ/ H_0) in minimum point (Fig.3.).

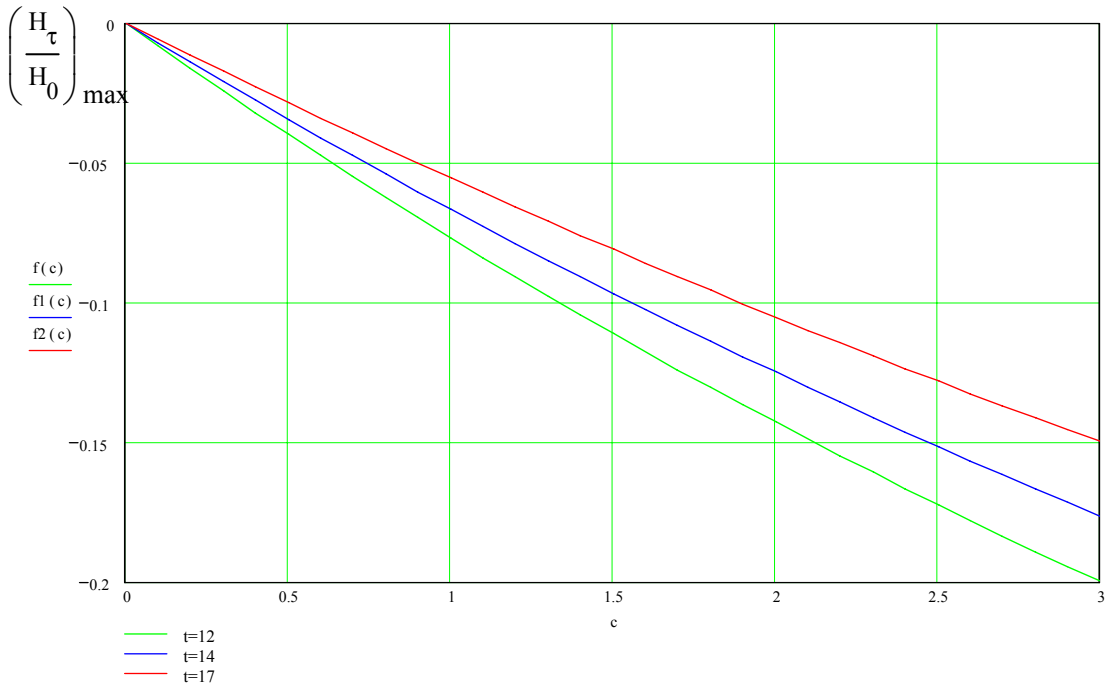

Fig.3.

To research the defect of welded joint of pore type the following model has been used:

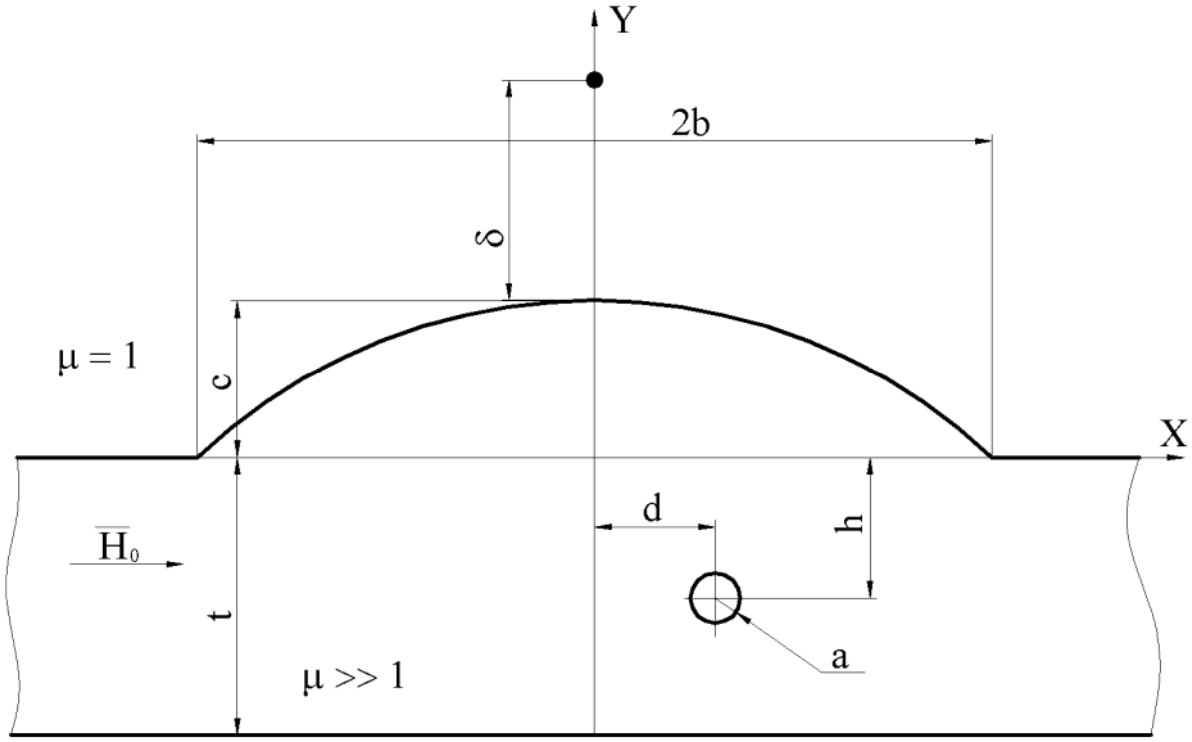

Fig.4.

where 2b - width of the strengthening welding joint bead,
c - height of the strengthening welding joint bead,
t – pipe's wall thickness,
δ - height of monitoring point
d – distance from pore to the axle of bead,
a – pore radius,
h – depth of pore bedding.

Fig.5 reflects the correspondence and distribution of magnetic field tangential component $H_{\tau d}/H_0$ for the pore type defects in the depth of seam considering the nonhomogeneity of magnetic field distribution in the seam:

$$\frac{H_\tau^d}{H_0'} + \frac{H_\tau}{H_0} = \frac{\left[\frac{1}{2}\cdot\frac{b^2}{c} - \frac{1}{2}\cdot c - \left[\left(\frac{1}{2}\cdot\frac{b^2}{c} + \frac{1}{2}\cdot c\right)^2 - x^2\right]^{\frac{1}{2}}\right]}{\left[t + \left[\left(\frac{1}{2}\cdot\frac{b^2}{c} + \frac{1}{2}\cdot c\right)^2 - x^2\right]^{\frac{1}{2}} - \frac{1}{2}\cdot\frac{b^2}{c} + \frac{1}{2}\cdot c\right]} - \frac{\left[t + \left[\left(\frac{1}{2}\cdot\frac{b^2}{c} + \frac{1}{2}\cdot c\right)^2 - x^2\right]^{\frac{1}{2}} - \frac{1}{2}\cdot\frac{b^2}{c} + \frac{1}{2}\cdot c\right]}{t} \cdot \frac{\left[2\cdot(x-d)^2 - (c+\delta+h)^2\right]}{\left[(x-d)^2 + (c+\delta+h)^2\right]^{\frac{5}{2}}} \cdot \frac{(\mu-1)}{(\mu+1)} \cdot a^3 \cdot \left[1 + \frac{(\mu-1)}{(\mu+1)} \cdot \left[1 - c^2 \cdot \frac{(c+h)^2}{b^4}\right]\right]$$

where:

- H_τ^d – field tangential component from the defect on the surface;
- H_0 - field value in the seam;
- d – displacement of pore from central Y-axis in direction of X-axis;
- μ - magnetic permeability of the seam material;
- a – pore radius;
- δ - height of monitoring point;
- h – depth of defect location.

Fig.5. When t=17mm, b=12 mm, c=2.5 mm, δ=2.5mm, h=5 mm, μ=240, a=1.5 mm, d=0.

Fig. 6, 7 reflect the distribution of magnetic field tangential component in the seam considering the depth of defect pore-type bedding and deviation of defect pore-type diameter.

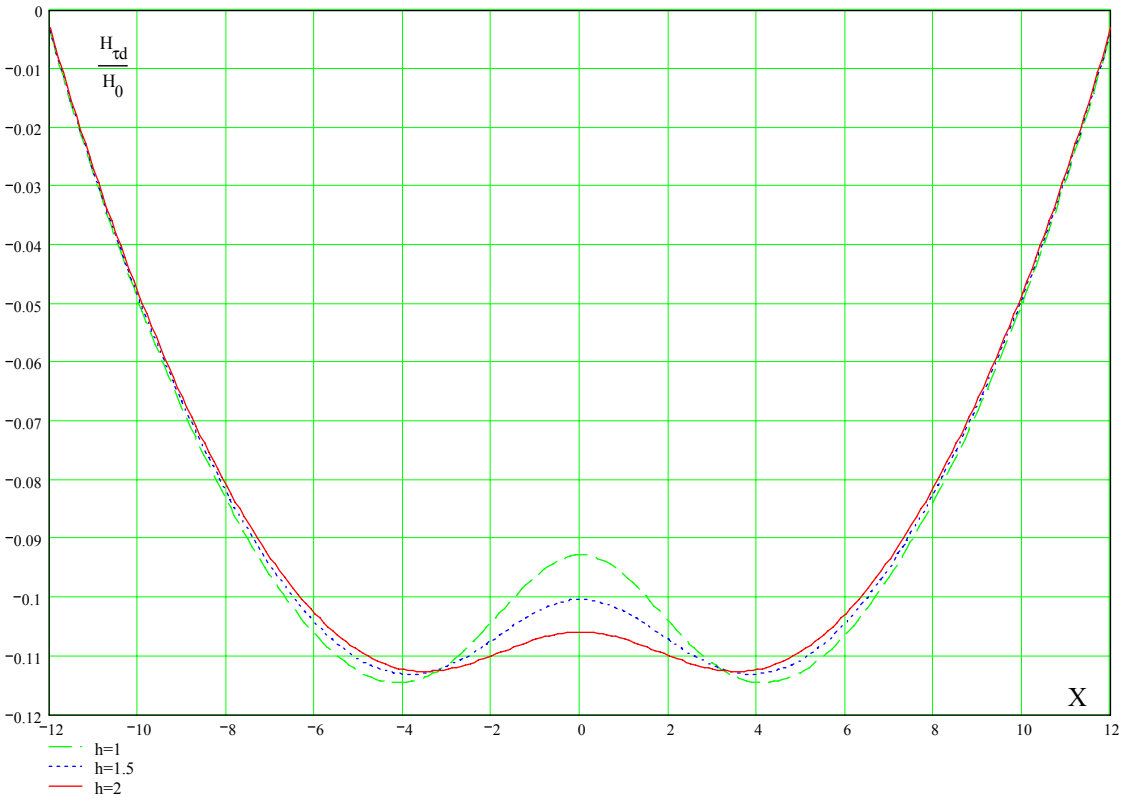

Fig.6. When h=1mm,1.5mm,2 mm.

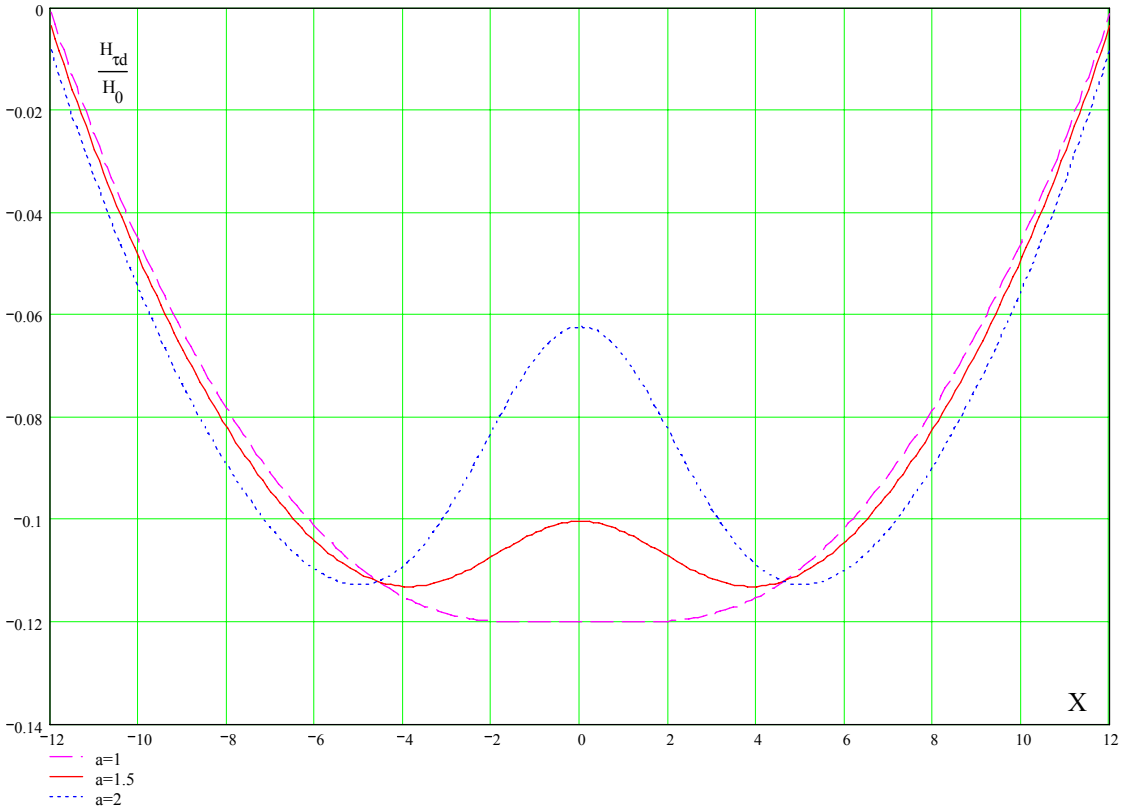

Fig.7. When h=1.5mm, a=1mm,1.5mm,2mm.

When displacing the pore from central Y-axis the distribution of magnetic field tangential component looks like on Fig.8:

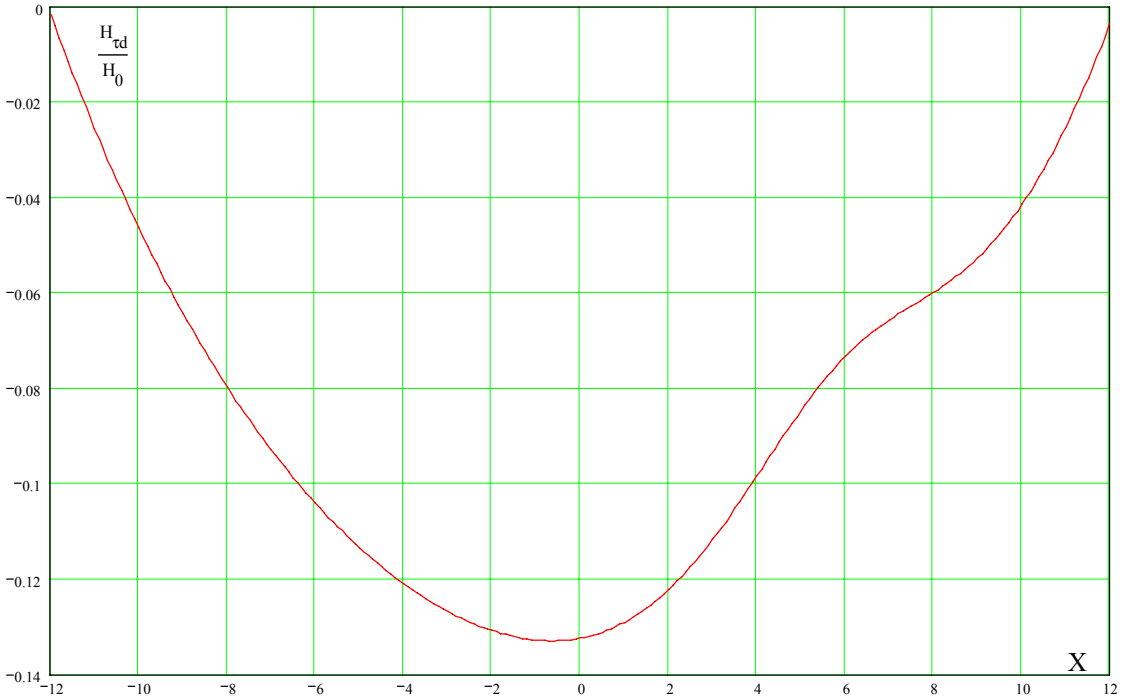

Fig.8. When d=6mm, h=5mm, a=1.5mm.

In order to research detectability of the pore type defect we will introduce k = a/h, where a – pore radius, h – depth of pore bedding.

Fig. 9 presents the correspondence between $H_{\tau max}$ for the pore type defect and parameter k. We can see that when $k \leq 0{,}25$ defect field H_τ^d doesn't influence in general on the distribution of magnetic field above the defect.

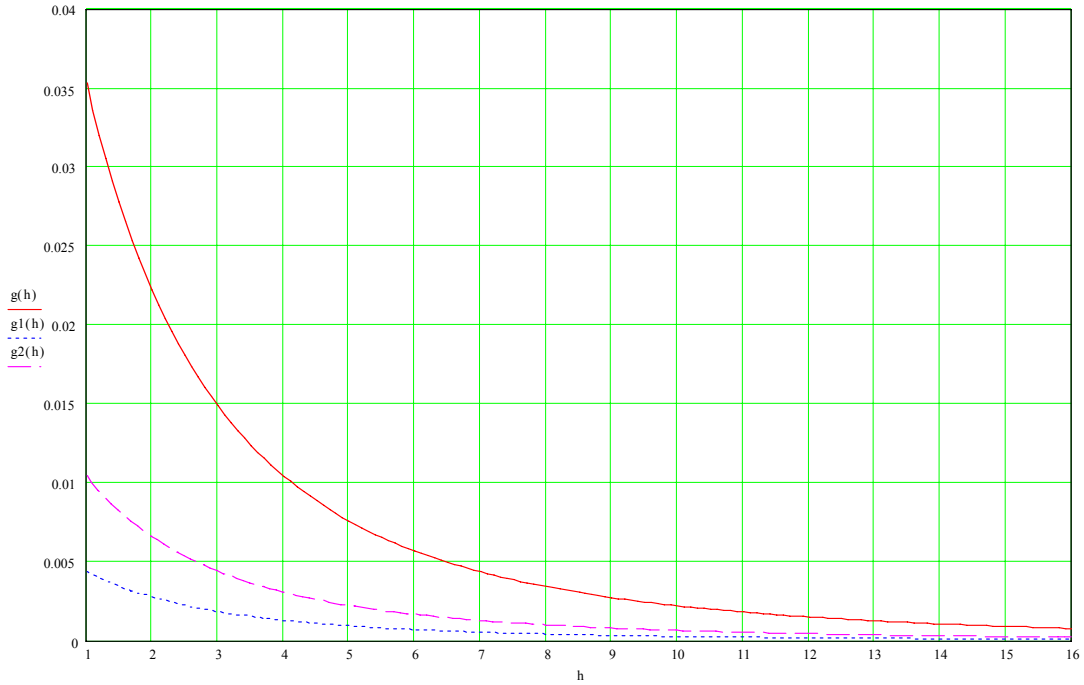

Fig.9.

Model for determining of correspondence of magnetic field tangential component for longitudinal crack in the seam is shown on Fig.10.

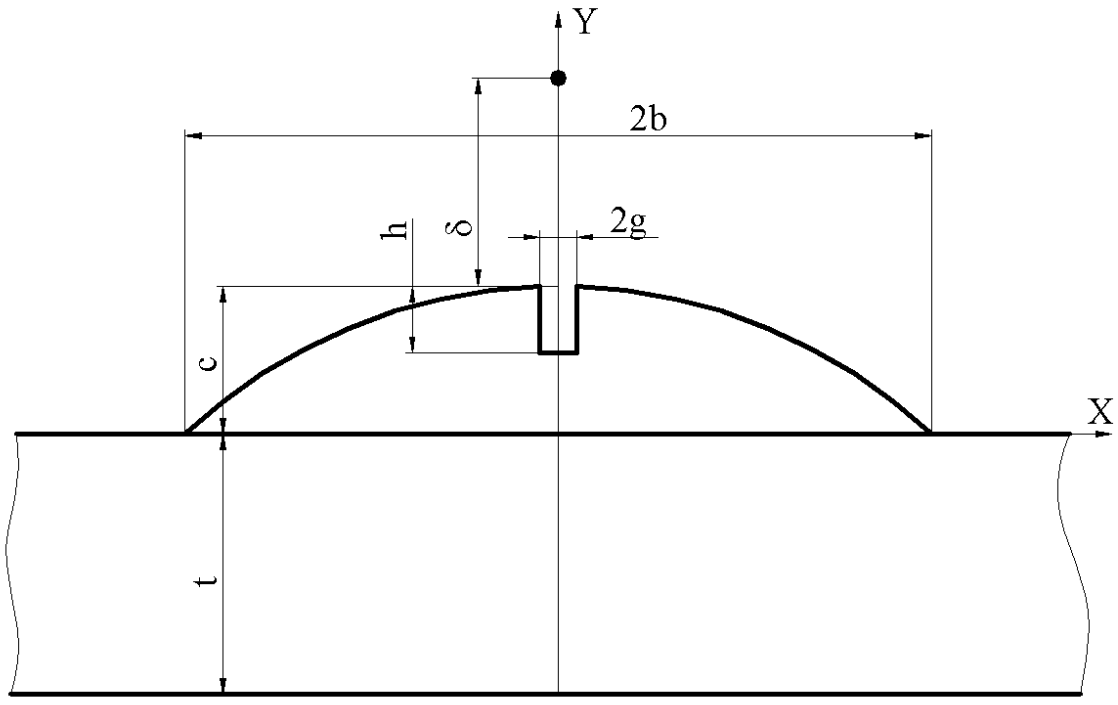

Fig.10.

Where:
2g – width of crack opening;
h – crack depth;

$$\frac{H_\tau^d}{H_0'} + \frac{H_\tau}{H_0} = \frac{\frac{b^2}{2\cdot c} - \frac{c}{2} - \sqrt{\left(\frac{b^2}{2\cdot c} + \frac{c}{2}\right)^2 - x^2}}{t + \sqrt{\left(\frac{b^2}{2\cdot c} + \frac{c}{2}\right)^2 - x^2} - \frac{b^2}{2\cdot c} + \frac{c}{2}} + \frac{\frac{h}{g} + 1}{\frac{h}{g} + \mu} \cdot \mu \cdot F02 \cdot \frac{g}{\pi} \cdot \frac{t}{t + \sqrt{\left(\frac{b^2}{2\cdot c} + \frac{c}{2}\right)^2 - x^2} - \frac{b^2}{2\cdot c} + \frac{c}{2}} \cdot \left[\frac{\delta - c}{x^2 + (\delta - c)^2} - \frac{\delta - c + h}{x^2 + (\delta - c + h)^2}\right]$$

$F_0 = 2{,}65$ – coefficient introduced by F. Ferster.

Distribution of magnetic field tangential component above the longitudinal crack type defect in correspondence with its depth in the seam is shown on Fig.11.

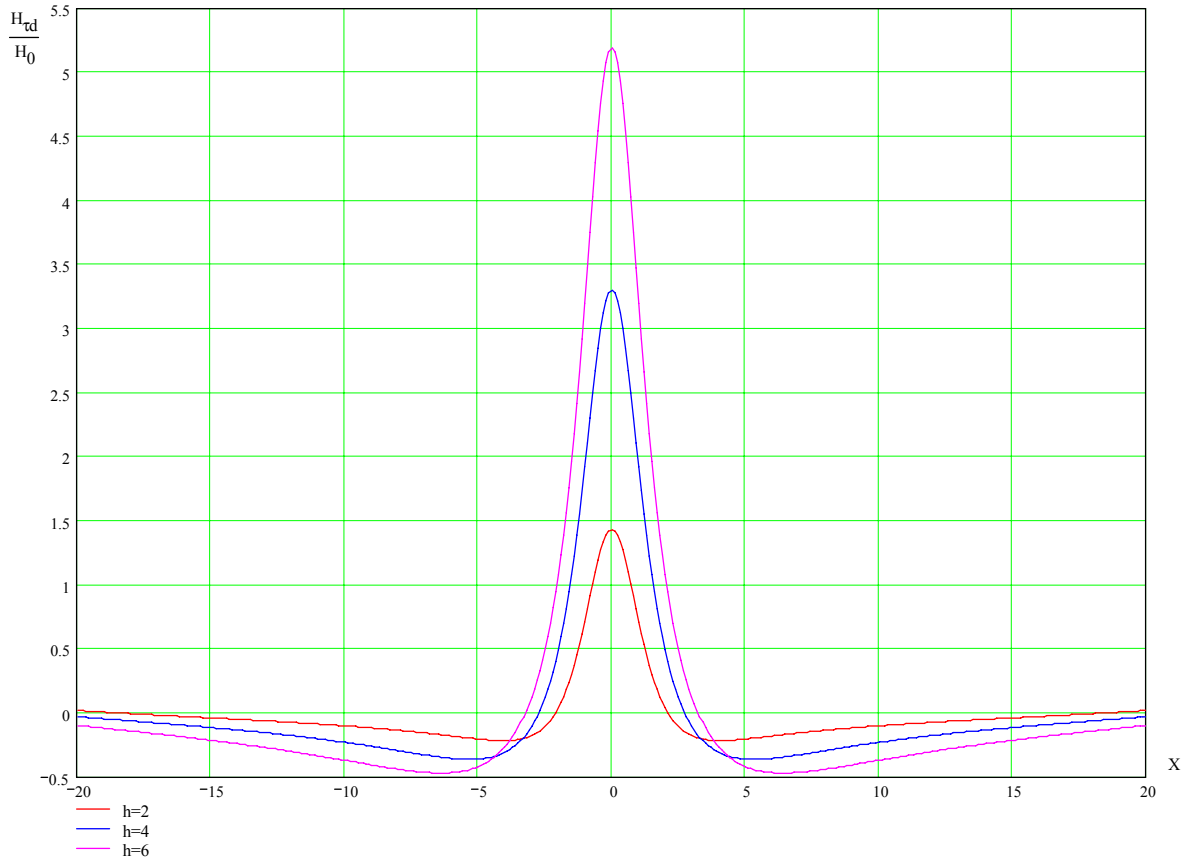

Fig.11. When t=16mm, b=16mm, c=1mm, δ=2.5mm, μ=240, g=0.5mm.

It is obvious from Fig.11, that the signal from the crack in the seam will be much stronger than the one from pore, i.e. using this method a small enough cracks can be detected.

Comparing distributions of tangential components for defects pore-type and longitudinal crack type we can see that maximal value of Hτ for longitudinal crack type significantly higher than maximal value of Hτ for pore-type defects.

Discussion

During prototyping the scanner "SkM-Sh" (Fig.12) we received the graphs of the field above the seam with the defect as well as without it (Fig.13).

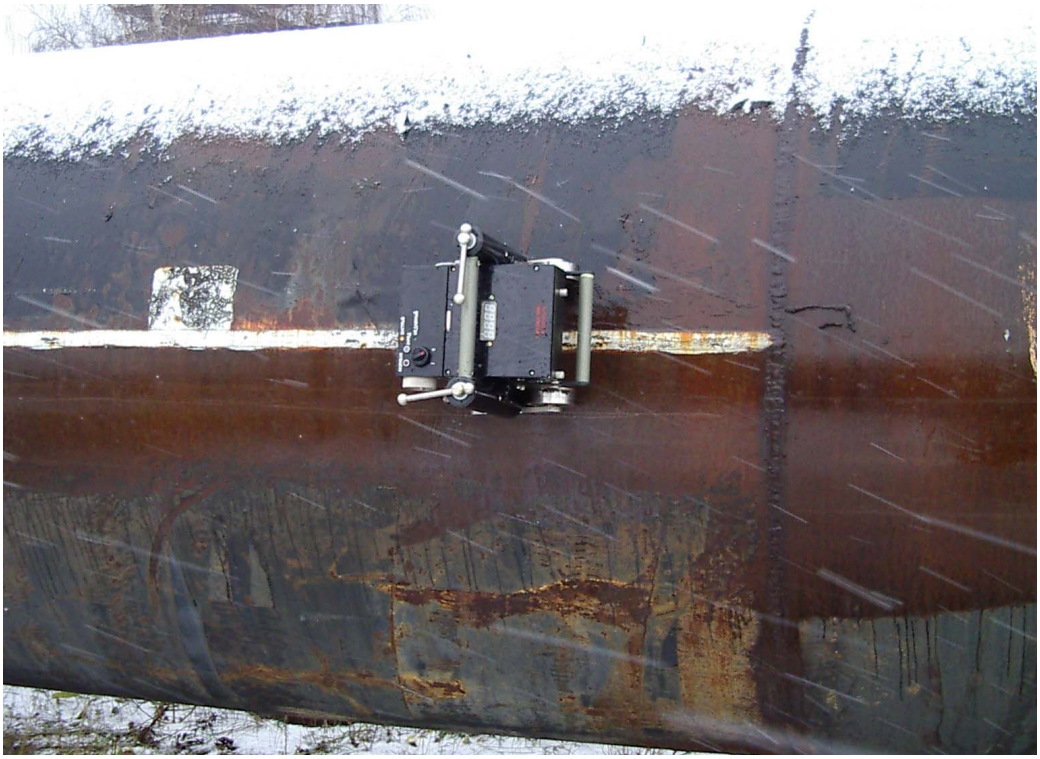

Fig.12. Scanner "SkM-Sh"

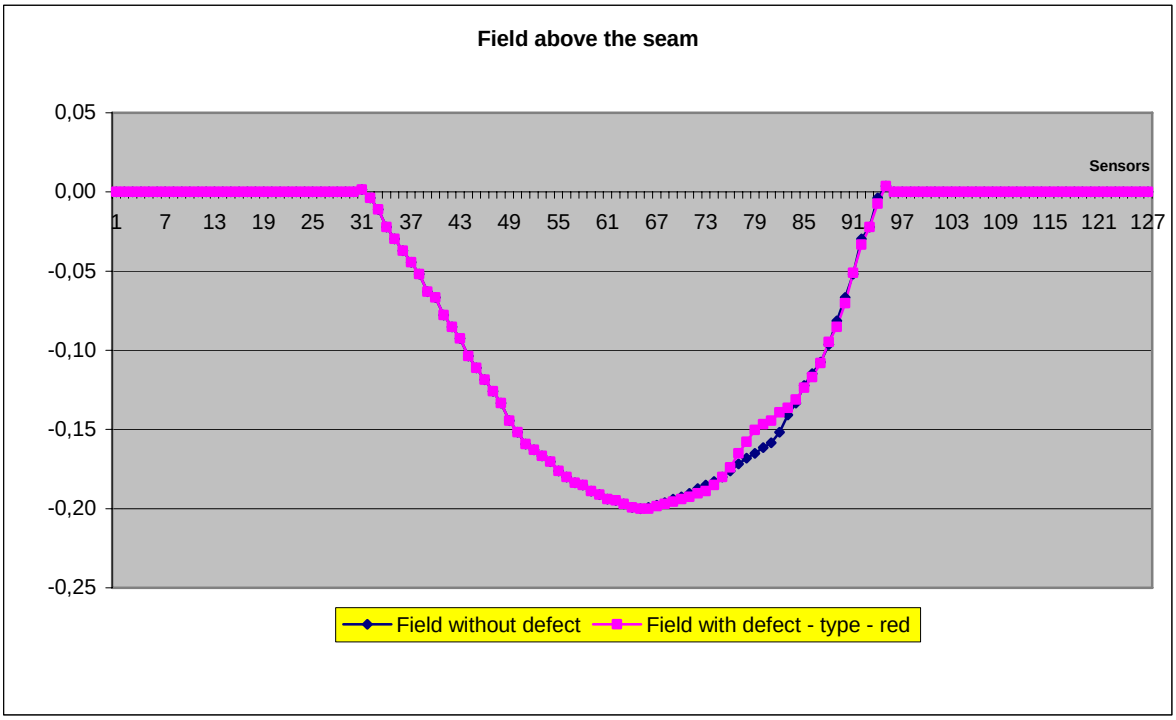

Fig.13. The seam field (without defect – blue, and with pore-type defect - red).

Comparing the theoretical curves of magnetic field distribution (Fig.8) with the curves received with the help of scanner we can determine the deviation in the values of data.
There are four curves shown on Fig.14.
Curve B – estimated field data above the seam without defect.
Curve A – estimated field data above the seam with defect.
Curve C – experimental field data above the seam with defect.
Curve D – experimental field data above the seam without defect.
Comparing and analyzing these curves we can conclude that:

- relative maximal deviation of determining the pore-type defect is 7%;
- relative maximal deviation of determining the signal from field above the seam is 13%.

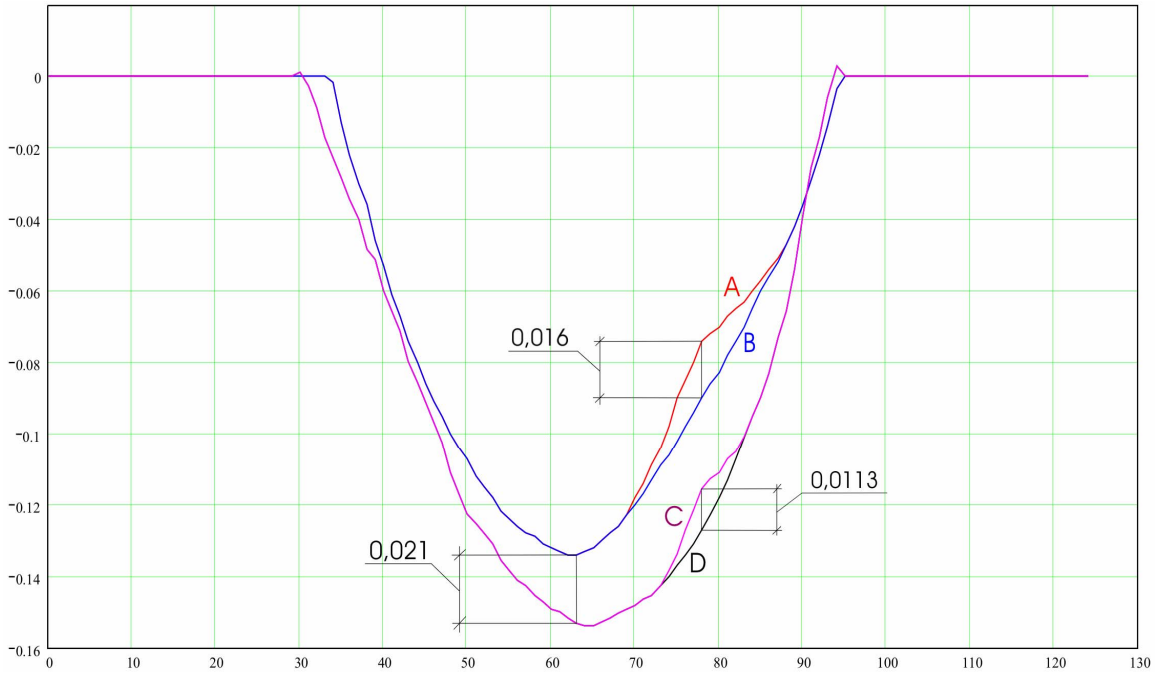

Fig.14. Comparison of theoretical and experimental data..

Analyzing the sensibility when determining the defects of welded joint a conclusion can be made that this method doesn't allow detecting all the pore-type defects.

When a/h ≤ 0,25 the field of the pore-type defect doesn't influence the general situation of magnetic field distribution above the defect,
where a – pore radius, h – depth of pore bedding.

I.e. for example when pore radius a=1 mm, its detectability will be guaranteed on a depth up to 4 mm from the outer surface of the pipe's wall. Maximal depth where the pore-type defect can be detected when a=3 mm is 12 mm.

Conclusions

As a result of this work we received mathematical models of welded joint considering nonhomogeneity of the field in the seam as well as models for the longitudinal crack type and for pore-type defects of the seam. These results form the base of working out the algorithms, design and software for scanners of welded joint "SkM-Sh" series.

Analysis of theoretical and experimental data allowed to determine the limits of magnetic method usage for monitoring welded joints. Basing on theoretical data an experimental sample of scanner which can determine defects in welded joints with high probability has been produced.